

Generation of Evenly-Spaced Pressure-Solution Seams During (Late) Diagenesis: A Kinetic Theory[†]

Enrique Merino¹, Peter Ortoleva^{1,2*} and Peter Strickholm¹

Departments of Geology¹ and Chemistry², Indiana University, Bloomington, Indiana 47405, USA

Abstract. Stylolites and pressure-solution seams can form during diagenesis of rocks subjected to stress through a feedback involving texture and pore-fluid solute concentration. This feedback destabilizes the state of uniform texture (represented here only by porosity, for simplicity). A mathematical kinetic model that includes pressure solution, diffusion, and reprecipitation predicts the spontaneous generation, even in initially uniform rocks, of regions alternatingly (in space) more and less soluble. A region that becomes more soluble also becomes simultaneously more porous. The kinetic theory predicts that stylolites can form at roughly constant spacings; this agrees with many field and petrographic observations. Bedding planes between beds that have initially different texture are shown by the theory to be the focus of a porosity instability that can lead to the formation of a stylolite and to the generation of more stylolites within each bed. This prediction agrees with the observation that many stylolites have developed at bedding planes.

Finally, the theory, on the basis of transport, kinetic and thermodynamic properties for calcite and quartz and their aqueous ions, predicts the order of magnitude of both the spacing between stylolites and their time of formation. For limestones the predicted spacing has a very large range, perhaps from 10^{-4} to 10^2 cm, and for quartz arenites, chert, and quartzites it is between 0.025 and 3 cm. These values agree crudely with spacings observed in rocks. The predicted times of formation of stylolites in quartzose rocks are not unreasonable: 6,300 to 1.7×10^6 years. The range of formation times for stylolites in limestones is very large due, as for the predicted spacings, to the sensitivity of both the solubility and growth/dissolution kinetics of calcite to pH, P_{CO_2} , and many inhibitors.

I. Introduction

A. Background

"Stylolites are partings between blocks of rock which exhibit complex mutual column and socket interdigitation"

[†] Work supported in part by a grant from the National Science Foundation

* A.P. Sloan Fellow, 1980-1982

Offprint requests to: E. Merino

(Dunnington 1967, p 340). They are roughly planar; can extend laterally for up to tens of meters or more; can branch into two; and may form any angle from 0 to 90° to the bedding. They are widespread in several types of sedimentary rocks, especially monomineralic ones (e.g., Pettijohn 1957, pp 213-217; Heald 1955; Amstutz and Park 1967; Park and Schot 1968). The interdigitations, or teeth, may be from a few micrometers to several tens of centimeters long; often have striations on their sides, and generally, but not always, are perpendicular to the main plane of the stylolite.

Several theories have been proposed to account for the generation of stylolites (see for example the summary given by Manten 1966), but the one accepted today is that they are produced by pressure solution after lithification - a theory already well argued by Stockdale (1922) for the Paleozoic limestones of southern Indiana, U.S.A. One important aspect of stylolitization is that it can considerably change the volume, thickness, and shape of sedimentary bodies (e.g., Dunnington 1967; Bathurst 1980). Another is that pressure solution may turn out to be the prime process to generate the solutes needed to account for the great amounts of cements observed in many sedimentary rocks (see for example Bjorlykke 1979; Bathurst 1980; Enos and Sawatsky 1981). Indeed, Wanless (1979) has shown that pressure solution can produce a whole spectrum of textures and structures, from stylolites to non-sutured seams to non-seam, pervasive pressure-solution features, depending on the amount of "insoluble" material contained in the initial rock and on its "structural resistance to change" (Wanless 1979, pp 438, 439 and 457).

In the genesis of stylolites by pressure solution there are several unsolved problems.

(1) It has long been puzzling that, in a rock having initially uniform texture and mineralogy, some regions are dissolved away (and become stylolites) while others are not (and become well cemented). How does a block of rock manage to respond to an overall applied stress by generating within itself regions of high solubility and regions of low solubility?

(2) One common feature of stylolites is their tendency to occur at regular distances in a slide, hand specimen, or outcrop. The regularity is of course crude, within a factor of 2 or 3 at most, but nevertheless real. For example, Heald (1955, p 104) mentions that "seams are generally 5-15 cm apart..." in the Pennsylvanian Pottsville sandstone; Purser (pers. comm., 1980) de-

scribes stylolites approximately every 10 cm in limestones of the Persian Gulf; Tremolières and Reulet (1978, Fig. 11a, b, c) show perfectly regular tectonic stylolites about 30 cm apart in Burdigalian limestones of southeastern France; Bathurst (1975, Fig. 325) also shows stylolites about 2–3 cm apart; and Alvarez et al. (1976) demonstrate that the strikingly periodic “fracture cleavage” (which they appropriately rename “spaced cleavage”) in Mesozoic limestones from northern Italy developed by pressure dissolution at and along regularly spaced surfaces. We ourselves have seen many excellent examples of evenly spaced stylolites in the Salem Limestone of south-central Indiana. How are regularly spaced stylolites generated?

(3) It will be argued below that stylolites develop, under the action of stress, from the textural heterogeneities, however small, that are ever present in rocks. However, how can a *planar* stylolite develop from what must be at least in some instances a *punctual* heterogeneity? How can that planar stylolite extend itself laterally even at an angle to the bedding, as is often the case?

(4) How are the column-and-socket interdigitations generated? Why are they not generated in the case of wavy or non-sutured seams?

The purpose of this paper is to propose a quantitative kinetic theory that accounts for (1) the spontaneous development of zones of pressure solution and cementation within rocks under stress, and (2) the generation of *regularly* spaced stylolites. We will show that the formation of stylolites and their common occurrence at roughly constant distances result directly from the kinetic interaction of pressure solution, transport of aqueous species away from the site of dissolution, and their reprecipitation elsewhere in the rock. Because the equations below only contain *one* spatial dimension (to simplify their numerical solution), our theory cannot therefore address the three-dimensional questions of how the interdigitations are generated and of how a point heterogeneity can become a planar feature (problems 4 and 3 above). Regarding the latter, Fletcher and Pollard (1981) have recently proposed the interesting idea that stylolites could be viewed as anticracks; their lateral propagation would then be akin to that of cracks.

Two aspects of stylolitization that have particular relevance to the theory discussed below are the distribution of porosity across a stylolite or set of stylolites and whether transport of pressure-dissolved ions is mainly by flow or by diffusion.

Dunnington (1967, p 342) pointed out that stylolites “... appear to have originated where porosities were originally highest but grain sizes were low.” Nevertheless, after stylolitization, porosity becomes lowest at and next to the stylolite along a line at right angles to it. This can be seen in the continuous porosity profiles¹ obtained by Harms and Choquette (1965, plate 3C), in the porosity logs given by Dunnington (1967, Figs. 4

and 9) for Cretaceous limestones of Qatar and Abu Dhabi, in the porosity measurements of Heald (1959, Table 1), and in the observations of Bathurst (1980, p 95) for the Maastrichtian gray chalk at Stevns Klint in Denmark. We suppose that the main cause for the minimum in porosity at the stylolite is the collapse, or physical displacement towards each other, of the two blocks of rock separated by a region of very high porosity – a collapse that is evidenced by the striations present on the sides of many stylolite teeth (Pettijohn 1957, p 215). We explain below how small regions having initially slightly-higher-than-average porosity become, under the action of stress, more and more porous at an accelerating rate. At a high enough porosity those regions collapse physically and their porosity becomes lowest.

As to the relative importance of flow and diffusion during stylolitization there are opposing views. For carbonates, Wanless (1979, pp 445, 458) and Buxton and Sibley (1981) favor flow, but Dunnington (1967, pp 340–342) argued convincingly that diffusion, not flow, is the dominant transport mechanism in removing the aqueous ions produced by pressure solution and thus in allowing stylolitization to continue. His reasons, recently reformulated and expanded by Bathurst (1980, pp 95–96), are

(1) The amount of rock mineral dissolved is greater than (though within an order of magnitude of) the amount of compactive fluid expelled; yet, at the pH's and P_{CO_2} 's in underground waters, transport by water flow of 1 cm³ of CaCO₃ requires 10³ to 10⁵ cm³ of very undersaturated water (and even more at temperatures >25°C, because the solubility of carbonates decreases with increasing temperature).

(2) The aqueous solution in a rock is bound to have been at least close to saturation even before pressure solution began, so that it could dissolve and carry away only the additional solubility caused by pressure solution.

On the other hand, however, externally imposed, non-compaction water flows could in principle account for the ionic transport required by pressure dissolution. The question in these cases is to identify independently that large enough flow rates and pressure gradients have indeed existed. At any rate, this paper refers to situations where diffusion dominates flow during stylolitization.

B. Qualitative Picture

In Sects. II–IV we develop a simplified kinetic theory of stylolitization, making for simplicity the following assumptions (though in the *Conclusions* we discuss ways to relax some of them):

- 1) all grains and pores are equant, and the grains have random orientations;
- 2) the rock is monomineralic;
- 3) the rock is subjected to a uniaxial stress;
- 4) nucleation is ignored;
- 5) the development of columns and sockets is left out;
- 6) also left out of the theory is the role of the direction of the stress in controlling the orientation of the stylolites;

¹ Harms and Choquette's (1965) gamma-ray method for continuous porosity determination is discriminating enough to tell apart differences in porosity at points as close to each other as 0.5 cm, a distance much smaller than the spacing between the stylolites studied by them

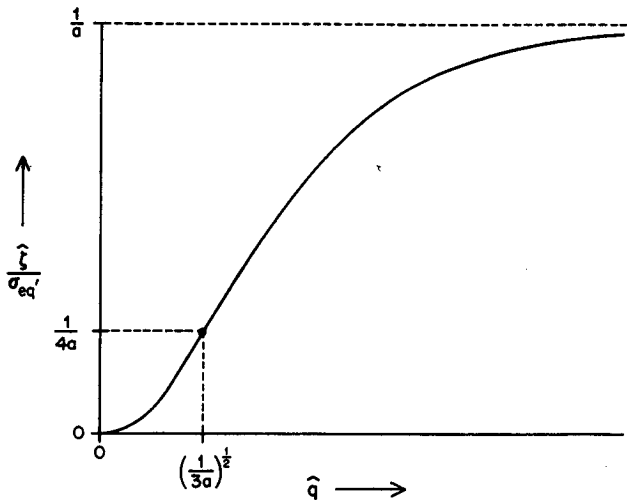


Fig. 1. Variation of ζ , the reciprocal of the exponential growth time, versus \hat{q} according to Eq. (IV.4); $(2\pi/\hat{q})$ is the pattern wavelength, or spacing between adjacent stylolites. $1/a \equiv (1 - \bar{\phi})^{2/3}$, where $\bar{\phi}$ is the average porosity. Equation (IV.4) is obtained through linear analysis of the stability of a stressed, homogeneous-texture rock to the formation of nonuniformity, as discussed in Sect. IV.A. Because ζ is positive for all \hat{q} , all patterns are expected to self-amplify. Thus, although the linear analysis shows that the system is unstable to stylolitization, it does not yield a characteristic length or range of lengths for the expected separation between adjacent stylolites. This expected spacing is found to be a nonlinear effect (see Sect. IV.B), and is shown in Figs. 2-4

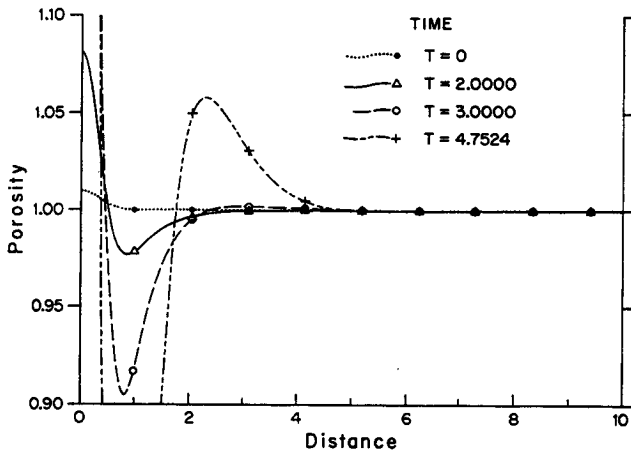


Fig. 2. Generation of a stylolite by porosity/pore fluid concentration feedback in a stressed rock having initially homogeneous texture with a small porosity deviation at the origin. The dynamics of the model proposed here naturally incorporates the coordinated genesis of parallel, regularly-spaced stylolites induced by a primary one. The process is described qualitatively in Sect. I.B. The graphs were generated by numerical solution of Eqs. (III.17, 18)

7) there is no externally imposed overall water flow through the rock.

Consider a one dimensional model of a monomineralic rock (such as limestone). Let us describe the rock by the concentration $X(r, t)$ of dissolved species in the pore fluid and the volume fraction $\phi(r, t)$ of pore space

(= porosity), where t is time and r is position along the rock. We assume the rock is subjected to a compressional stress in the r -direction.

The central postulate of our theory is that the free energy of an individual crystal depends on the local texture - here characterized by the porosity. We adopt a mean-field approach (Ortoleva et al. 1982) in which a typical crystal should be at a higher stress-strain energy if, because of a larger local porosity, it has to carry a larger burden of the load (Dunnington 1967, p342). This suggests that the equilibrium concentration of component dissolved in the pore-fluid should depend on the local porosity. The main feature of the theory proposed is thus the feedback between the porosity and the pore-fluid composition.

For the one dimensional system this implies that a local porosity fluctuation, as seen for example in Fig. 2, will tend to self-amplify: the grains in a region of higher porosity must bear a higher load per grain; this raises the equilibrium concentration in the pore fluid for this region; diffusion or other transport then takes this material away to regions of the rock where ϕ is lower; but this leads to further dissolution, and the process runs away.

Interestingly, we see in Fig. 2 that a local porosity maximum not only self-amplifies, but also induces satellite maxima. This occurs because the primary ϕ maximum causes the adjacent rock to become cemented due to the increase of the pore concentration above the neighboring equilibrium value. This induced porosity minimum thus becomes a region of lower equilibrium concentration than the region further from the original ϕ maximum, and this clearly brings about a secondary ϕ maximum. A single stylolite can therefore induce a well ordered sequence of satellite stylolites, such as those commonly observed.

In the next section we turn these qualitative arguments into a mathematical model.

II. A Simple Porosity-Feedback Stylolitization Model

The model developed here is similar to the texture dynamic theory set forth by Ortoleva et al. (1982). In that work we proposed coupling equations for the texture, rock flow and composition of the intergranular fluid. Here we apply our considerations to a monomineralic, porous rock.

In any given region of space we describe the rock by the density of crystals n (number of crystals per unit volume), the volume of the typical crystal L^3 (assumed equant for simplicity) and the volume fraction ϕ of the pore space. These quantities are related by

$$nL^3 + \phi = 1 \quad (\text{II.1})$$

stating that the volume fraction of pores plus that of crystals (nL^3) must be unity.

We envision the formation of a stylolite to involve two processes. The first is an amplification of local porosity maxima and minima through the action of anisotropic stresses. The second consists of an overall compaction and/or collapse of the rock that occurs in the regions of porosity maxima. The latter processes are much more complex and usually involve local shortening (flattening) of the grains in the compaction di-

reaction because of preferential pressure dissolution. These two processes are not necessarily separated in time. We characterize the first process as an evolution wherein the rock does not compact appreciably but the porosity distribution changes, and shall limit our treatment to that case only. Thus, neglecting nucleation, we may assume that the number of crystals per unit volume n does not change in time and will furthermore be taken to be constant in space.

Let \mathcal{G} represent the rate of volume change of a grain

$$\frac{\partial L^3}{\partial t} = \mathcal{G}. \quad (\text{II.2})$$

Using (II.1) and the constancy of n we thus get

$$\frac{\partial \phi}{\partial t} = -n\mathcal{G}. \quad (\text{II.3})$$

Next let X be the concentration (per rock volume) of dissolved component. The reaction-transport equation takes the form

$$\frac{\partial X}{\partial t} = -\vec{v} \cdot \vec{J} - \rho n \mathcal{G} \quad (\text{II.4})$$

where ρ is the molar density of the mineral and \vec{J} is the (vectorial) flux of dissolved component. We now complete the theory by postulating the dependence of \mathcal{G} and \vec{J} on our descriptive variables X and ϕ .

For a system free of pore fluid flow we assume a Fick-type transport law

$$\vec{J} = -D(\phi) \vec{\nabla}(X/\phi). \quad (\text{II.5})$$

The porosity dependence of D is usually taken to be of the form (Berner 1980; Lerman 1979)

$$D(\phi) = D_c \phi^m \quad (\text{II.6})$$

where $3/2 \lesssim m \lesssim 2$ and D_c is the diffusion coefficient in bulk fluid. It is the gradient of the concentration per pore volume X/ϕ , and not of X , that drives diffusion; hence we have written (II.5).

The growth or dissolution rate \mathcal{G} must be proportional to the crystal surface area and thus proportional to L^2 . The rate of addition to the crystals is taken to be proportional to the concentration of dissolved component *per pore volume*, X/ϕ . (This assumes that the mineral dissolves into only *one* aqueous species, $A \rightleftharpoons X$, which is true for quartz but not for calcite. When the mineral dissolves into two or more species the rate law (II.7) should be extended like in Strickholm et al. 1983.) Hence we take the rate of addition in the form $L^2 k X/\phi$, where k is a rate coefficient (that differs from the usual one by a geometrical factor of order 6, because the grain's area is $\sim 6L^2$, not L^2). Writing the dissolution rate in the form $L^2 k X^{eq}(\phi)/\phi$ we obtain

$$\mathcal{G} = \frac{kL^2}{\phi \rho} \{X - X^{eq}(\phi)\}. \quad (\text{II.7})$$

Finally L can be eliminated from (II.7) via (II.1) to obtain

$$\mathcal{G}(X, \phi) = \frac{k(1-\phi)^{2/3}}{n^{2/3} \phi \rho} \{X - X^{eq}(\phi)\}. \quad (\text{II.8})$$

When the applied stress is turned off, $X^{eq}(\phi) = \phi c_0^{eq}$ where c_0^{eq} is the equilibrium concentration of dissolved component in moles per pore volume. For a rock under stress, $X^{eq} = \phi c^{eq}(\phi)$ where $c^{eq}(\phi)$ is expected to be a monotonically increasing function of ϕ . The actual calculation of $c^{eq}(\phi)$ is a difficult problem in the theory of random media (Ortoleva et al. 1982 and references therein), but the pressure solution aspects of the two-grain problem have been studied recently by Rutter (1976) and Robin (1978). In the present study, however, we take a simple phenomenological approach as follows. For a one dimensional system, each crystal should be subjected to a local stress that is proportional to the applied overall stress divided by the surface area between grains. The latter is, on the average, proportional to the square of the fraction of the total surface area occupied by crystals as seen in a slice through the rock. This fraction f is equivalent to the volume fraction of crystals, as can be shown by taking a thin cross-sectional slab and letting its thickness go to zero. Thus f is simply given by

$$f = 1 - \phi. \quad (\text{II.9})$$

We next write c^{eq} in the suggestive form

$$c^{eq} = c_0^{eq} e^{\Delta\mu/RT} \quad (\text{II.10})$$

where R is the gas constant, T is the absolute temperature and $\Delta\mu$ is the excess molar free energy of the crystal under the local stress. To proceed further we invoke Kamb's (1959) theory of the equilibrium properties of stressed crystals. He showed that the change in chemical potential $\Delta\mu$ from the non-stressed to the stressed crystal depends on the crystal-facet orientation and the direction and type (shear or compressional) of applied stress. Because our description of the rock is not so detailed, we consider $\Delta\mu$ as a facet-averaged quantity. From Kamb's theory, $\Delta\mu$ is expected to have contributions linear and quadratic in the applied stress, denoted α' and β' , respectively. That is, $\Delta\mu = \alpha' + \beta'$ (α' and β' being calculated using the macroscopic applied stresses), and then

$$\Delta\mu = \frac{\alpha''}{f^2} + \frac{\beta''}{f^4}, \quad (\text{II.11})$$

where we have added the second primes on α and β to incorporate possible statistical and geometric factors (of order unity) that might arise in a more rigorous treatment of the random crystal aggregate.

(II.11) then becomes

$$c^{eq}(\phi) = c_0^{eq} \exp \left\{ \frac{\alpha}{f^2} + \frac{\beta}{f^4} \right\} \quad (\text{II.12})$$

where

$$\alpha = \alpha''/RT, \quad \beta = \beta''/RT \quad (\text{II.13})$$

are constants. A more explicit calculation of α and β from thermodynamic data is deferred until Sect. V. Note that as $\phi \rightarrow 1$ (the rock being all dissolved away) $c^{eq} \rightarrow \infty$ (the individual crystals are under exceedingly high stress) and hence the rate of dissolution, $L^2 k c^{eq}$, diverges. Before this happens, however, the rock will fail or collapse. The present model is studied first to focus on the positive feedback nature of the process. Indeed, much before $\phi \rightarrow 1$, the monotonic increase of c^{eq} with ϕ in (II.12) will cause the local dissolution runaway that drives spontaneous stylolite formation in our model, satisfying our objective of explaining stylolite formation.

To summarize, the mathematical description of our model consists of the X , ϕ dynamics (II.3, 4) with pore diffusion (II.5, 6) and a crystal growth rate $\mathcal{G}(\phi, X)$ given by (II.8, 10, 12). In the next sections we shall discuss the physical consequences of these equations.

III. Scaling and Essential Parameters

It is essential to recast the simple model in such a way that characteristic times and lengths can be made explicit. Here we do this in two steps. First we introduce a preliminary set of dimensionless variables and then we introduce explicitly the parameters of the dependence of c^{eq} on ϕ so as to get a more precise handle on the characteristic times and lengths in the problem.

A. Preliminary Nondimensionalization

The concentration of mobile component (moles per pore volume) is much smaller than the solid molar density ρ by a factor denoted ε that is typically (for carbonates and silicates) on the order of 10^{-2} to 10^{-6} . In recasting Eqs. (II.3, 4) we make this smallness parameter explicit. We also introduce dimensionless concentration γ , space s , and time τ according to

$$\begin{aligned} t &= t_c \tau / \varepsilon, \\ r &= \sqrt{D_c t_c} s, \\ X &= \varepsilon \rho \phi \gamma, \\ t_c &= (k n^{1/3})^{-1}, \\ \varepsilon &= c_0^{eq} / \rho. \end{aligned} \quad (III.1)$$

With these new variables defined in (III.1) the X , ϕ Eqs. (II.3, 4) take the form

$$\varepsilon \phi \frac{\partial \gamma}{\partial \tau} = \frac{\partial}{\partial s} \left(\phi^m \frac{\partial \gamma}{\partial s} \right) - (1 - \phi)^{2/3} (\gamma - \gamma^{eq}) (1 - \varepsilon \gamma), \quad (III.2)$$

$$\frac{\partial \phi}{\partial \tau} = -(1 - \phi)^{2/3} (\gamma - \gamma^{eq}). \quad (III.3)$$

Here the scaled dimensionless equilibrium concentration γ^{eq} is defined by

$$c^{eq}(\phi) = \varepsilon \rho \gamma^{eq}(\phi). \quad (III.4)$$

Hence, from (II.12) we see that

$$\gamma^{eq}(\phi) = \exp \left\{ \frac{\alpha}{f^2} + \frac{\beta}{f^4} \right\}. \quad (III.5)$$

B. Mechanistic Scaling

The preliminary scaling resulting in (III.2, 3) is not complete because it makes no account of the particularities of the mechanism, i.e. α , β and f in (III.5), in determining the length and time scales appropriate to the system. To see how these enter in physically interesting cases, we seek the behavior of the dynamics near the initial phase where ϕ is fairly small at all points in the system. From III.5 and II.9 we obtain

$$\gamma^{eq} = \exp \left\{ \frac{\alpha}{(1 - \phi)^2} + \frac{\beta}{(1 - \phi)^4} \right\} \underset{\phi \rightarrow 0}{\sim} e^\lambda [1 + (2\alpha + 4\beta)\phi] \quad (III.6)$$

where

$$\lambda = \alpha + \beta. \quad (III.7)$$

Thus if $\bar{\phi}$ is the mean porosity then we expect that $e^\lambda (2\alpha + 4\beta) \bar{\phi}$ is a typical value for the stress-induced supersaturation. Since it is this stress-induced oversaturation that causes pattern formation in the present theory, we emphasize this quantity by introducing the following definitions:

$$\gamma = e^\lambda [1 + \omega \sigma] \quad (III.8)$$

$$\gamma^{eq} = e^\lambda [1 + \omega \sigma^{eq}(\Psi)] \quad (III.9)$$

$$\phi = \bar{\phi} \Psi \quad (III.10)$$

$$\omega = (2\alpha + 4\beta) \bar{\phi}. \quad (III.11)$$

From (III.9, 5, 7) we get

$$\sigma^{eq}(\Psi) = \left[\exp \left(\frac{\alpha}{f^2} + \frac{\beta}{f^4} \right) - \exp(\alpha + \beta) \right] / \omega \exp(\alpha + \beta). \quad (III.11a)$$

From its definition $\sigma^{eq}(\Psi) \rightarrow \Psi$ as Ψ (or ϕ) $\rightarrow 0$. We introduce a new dimensionless time $\hat{\tau}$ and space \hat{s} via

$$\tau = \bar{\tau} \hat{\tau}, \quad s = \bar{s} \hat{s} \quad (III.12)$$

where the quantities $\bar{\tau}$ and \bar{s} are to be determined. (III.2, 3) become

$$\frac{\bar{\phi}}{\bar{\tau}} \frac{\partial \Psi}{\partial \hat{\tau}} = -\omega e^\lambda (1 - \bar{\phi} \Psi)^{2/3} [\sigma - \sigma^{eq}(\Psi)], \quad (III.13)$$

$$\begin{aligned} \varepsilon \frac{\bar{\phi}}{\bar{\tau}} \Psi \frac{\partial \sigma}{\partial \hat{\tau}} &= \frac{\bar{\phi}^m}{\bar{s}^2} \frac{\partial}{\partial \hat{s}} \left(\Psi^m \frac{\partial \sigma}{\partial \hat{s}} \right) - (1 - \bar{\phi} \Psi)^{2/3} [\sigma - \sigma^{eq}(\Psi)] \\ &\quad \cdot [1 - \varepsilon e^\lambda (1 + \omega \sigma)]. \end{aligned} \quad (III.14)$$

From (III.13) we see that the natural choice for $\bar{\tau}$ is

$$\bar{\tau} = \frac{\bar{\phi}}{\omega e^\lambda}. \quad (III.15)$$

In order to remove as many parameters as possible from the equations, we define \bar{s} via

$$\bar{s} = \bar{\phi}^{m/2} \quad (III.16)$$

and (III.13, 14) become

$$\frac{\partial \Psi}{\partial \hat{\tau}} = -(1 - \bar{\phi} \Psi)^{2/3} [\sigma - \sigma^{eq}(\Psi)] \quad (III.17)$$

$$B\Psi \frac{\partial \sigma}{\partial \hat{t}} = \frac{\partial}{\partial \hat{s}} \left(\Psi^m \frac{\partial \sigma}{\partial \hat{s}} \right) - (1 - \bar{\phi}\Psi)^{2/3} [\sigma - \sigma^{eq}(\Psi)] \cdot [1 - \varepsilon e^\lambda (1 + \omega \sigma)]. \quad (\text{III.18})$$

The constant B is defined by

$$B = \frac{\varepsilon \bar{\phi}}{\bar{\tau}} = \varepsilon \omega e^\lambda. \quad (\text{III.19})$$

For small ε and $\bar{\phi}$ this system of equations turns out to have the same mathematical structure as the one that appears in modeling precipitation patterns (Feeney et al. 1983). It was found there by numerical solution that the characteristic length scale of patterns that arise in this system of equations is on the order of 4, a value that turns out to be independent of B for small B .

In summary, we expect the spatial patterning to take place on a scale given by combining (III.1) and (III.16). Denoting this characteristic length R_c we have

$$R_c = \bar{s} \sqrt{D_c t_c} = (D_c \bar{\phi}^m / k n^{1/3})^{1/2}. \quad (\text{III.20})$$

The characteristic time for developing this pattern, T_c , is expected to be

$$T_c = t_c \bar{\tau} / \varepsilon = [2 \varepsilon k (\alpha + 2\beta) n^{1/3} e^{(\alpha + \beta)}]^{-1}. \quad (\text{III.21})$$

The average porosity $\bar{\phi}$ enters (III.20) but not (III.21), implying that smaller $\bar{\phi}$'s lead to smaller stylolite spacings but do not change their time of formation. The stress applied enters (through α and β) the expression for T_c but not that for R_c ; this suggests that *any* stress, however small, will produce stylolites if it operates long enough, that is, if it operates over a time T_c , which does become longer the smaller the stress is.

IV. Instability to Stylolitization

We now show explicitly that the present model possesses instability to the formation of stylolites via a linear stability analysis and numerical solutions of the full nonlinear dynamics.

A. Linear Stability Analysis

In order for the stressed system spontaneously to generate stylolites from an initially macroscopically uniform texture, small deviations from uniformity must grow. Thus we now study the temporal development of small deviations $\delta\Psi = \Psi - 1$, $\delta\sigma = \sigma - \sigma_{eq}(1)$ from the uniform state $\bar{\Psi} = 1$, $\bar{\sigma} = \sigma_{eq}(1)$. Neglecting quadratic and higher order terms in $\delta\sigma$, $\delta\Psi$ in (III.17, 18) and dropping the small B and ε terms in (III.18) we obtain

$$\frac{\partial \delta\Psi}{\partial \hat{t}} = -(1 - \bar{\phi})^{2/3} [\delta\sigma - \sigma'_{eq} \delta\Psi], \quad (\text{IV.1})$$

$$0 = \frac{\partial^2 \delta\sigma}{\partial \hat{s}^2} - (1 - \bar{\phi})^{2/3} [\delta\sigma - \sigma'_{eq} \delta\Psi], \quad (\text{IV.2})$$

where $\sigma'_{eq} \equiv (\partial \sigma_{eq} / \partial \Psi)_{\Psi=1}$. It is easy to show that these equations yield solutions of the form

$$\begin{aligned} \delta\Psi &= A \sin(\hat{q}\hat{s}) \exp(\hat{\zeta}\hat{t}), \\ \delta\sigma &= B \sin(\hat{q}\hat{s}) \exp(\hat{\zeta}\hat{t}) \end{aligned} \quad (\text{IV.3})$$

where $2\pi/\hat{q}$ is the wavelength and $(\hat{\zeta})^{-1}$ is the exponential growth time (in the \hat{s} , \hat{t} space-time). Substituting (IV.3) into (IV.1, 2) we find

$$\begin{aligned} [-\hat{\zeta} + (1 - \bar{\phi})^{2/3} \sigma'_{eq}] A - (1 - \bar{\phi})^{2/3} B &= 0, \\ (1 - \bar{\phi})^{2/3} \sigma'_{eq} A - [\hat{q}^2 + (1 - \bar{\phi})^{2/3}] B &= 0. \end{aligned} \quad (\text{IV.3a})$$

The condition for the solutions (IV.3) to be non-trivial is that the determinant of the matrix of the coefficients of A and B in (IV.3a) be zero, which yields

$$\begin{aligned} [-(1 - \bar{\phi})^{2/3} \sigma'_{eq} + \hat{\zeta}] [\hat{q}^2 + (1 - \bar{\phi})^{2/3}] \\ + (1 - \bar{\phi})^{4/3} \sigma'_{eq} &= 0, \end{aligned} \quad (\text{IV.3b})$$

from which

$$\hat{\zeta}(\hat{q}) = \frac{\sigma'_{eq} \hat{q}^2}{1 + (1 - \bar{\phi})^{-2/3} \hat{q}^2}. \quad (\text{IV.4})$$

Since the equilibrium concentration increases with porosity, $\sigma'_{eq} > 0$. Hence $\hat{\zeta} > 0$, and the $\delta\Psi$, $\delta\sigma$ perturbations grow exponentially in time - i.e., the macroscopically stressed, uniformly-textured porous rock is unstable to the development of porosity differences.

Equation (IV.4) is shown in Fig. 1. $\hat{\zeta}$ is always > 0 , and is a monotonically increasing function of \hat{q} . Thus the smallest wavelength modes (i.e., those with largest \hat{q}) are the most rapidly growing, because they have the largest $\hat{\zeta}$. Of course, physically our theory only holds for length scales greater than $n^{-1/3}$, which is approximately the grain size for small porosity. It is not clear, therefore, from the present linear analysis what the preferred length scale for stylolite separation actually is. To address this point and to show how the longer wavelength modes can dominate even though the smaller wavelength modes are the fastest growing we now turn to the numerical simulation of the full nonlinear problem.

B. Numerical Simulations

We now present numerical simulations of the porosity evolution equations developed in the previous section. The numerical integration of (III.17, 18) is carried out for a one dimensional system. The spatial coordinate, fixing position, is limited to the interval

$$0 \leq \hat{s} \leq \hat{s}_m. \quad (\text{IV.5})$$

We assume no losses of mobile component out the ends; thus

$$\frac{\partial \sigma}{\partial \hat{s}} = 0 \quad \text{at} \quad \hat{s} = 0, \hat{s}_m. \quad (\text{IV.6})$$

The system evolution from a given initial data $\sigma(\hat{s}, 0)$ and $\Psi(\hat{s}, 0)$ is approximated using an iterated backward difference technique (von Rosenberg 1969). To minimize rapid initial transients, the initial data are constructed by picking a given $\Psi(\hat{s}, 0)$ and then letting $\sigma(\hat{s}, 0) = \sigma^{eq}(\Psi(\hat{s}, 0))$.

1. *Induction of satellite stylolites.* Several types of initial data were considered. In one sequence the system was

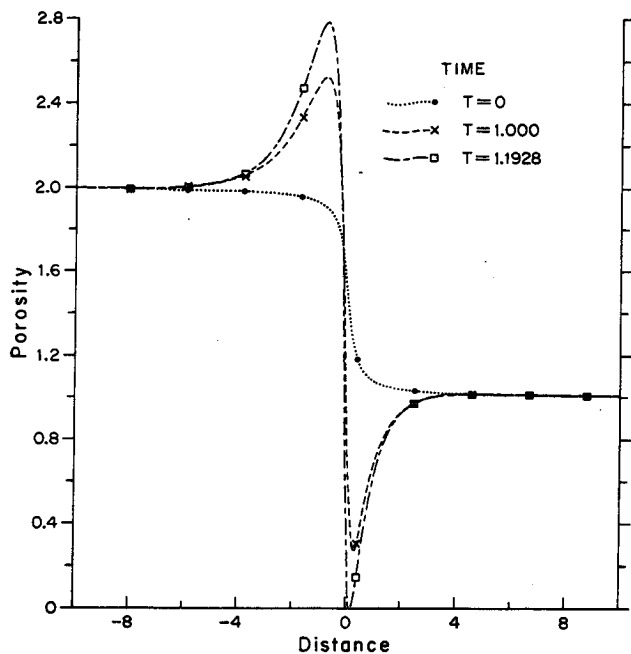


Fig. 3. Generation of stylolites at the boundary between regions having initially contrasting porosity in a stressed rock. The stylolite spacing is shorter than the thickness of the beds having initially different porosity. The evolution is controlled by the porosity/pore-fluid concentration dynamics developed in Sects. II and III. The graphs shown here are obtained by numerical solution of Eqs. (III.17, 18)

started with a small porosity deviation superimposed on a constant background to model a small local inhomogeneity, always present in any natural system. The results, shown in Fig. 2, demonstrate the induction of satellite porosity maxima, discussed qualitatively in Sect. IB. From this we see that pressure solution coupled to transport leads to amplification of porosity variations and regular patterns. The role of the initial porosity bump can be played by some small non-uniformity in the rock: similar results would follow if one of the walls represented an interface between two lithologies or two formations with different textures or compositions.

2. Case of two beds with initial porosity differences.

Here the initial porosity difference ($\Psi(\xi, 0)$) will be accentuated when a stress is applied. As can be seen in the simulation of Fig. 3, the porosity difference is first enhanced, and a stylolite first develops, at the region of rapid change of porosity - the bedding plane. Then satellite stylolites are produced sequentially within the beds. The proposed theory assigns therefore both a time and a place for the formation of each stylolite. The predicted location of stylolites at bedding planes is observed often.

3. Evolution of random texture deviations.

The sedimentary rocks in which many stylolites develop are monomineralic (Pettijohn 1957, p 214) and, through the previous action of sedimentary processes, tend to have a texture describable in terms of a "rock average" texture on which are superimposed relatively small, random

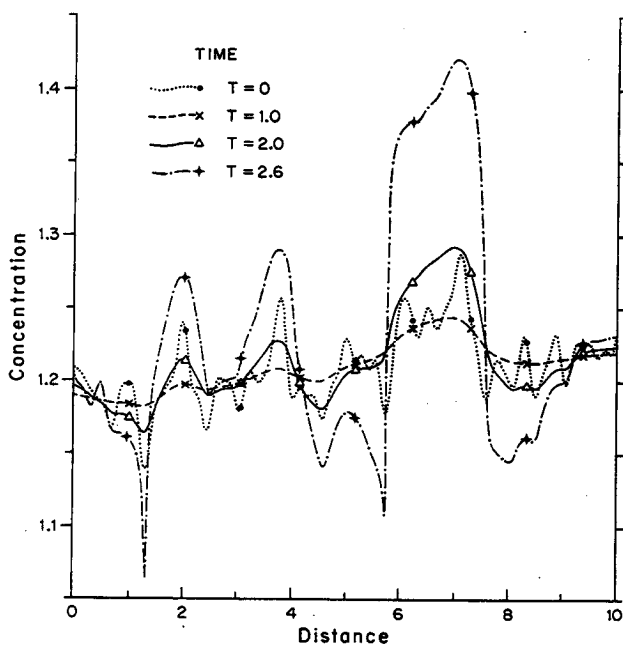
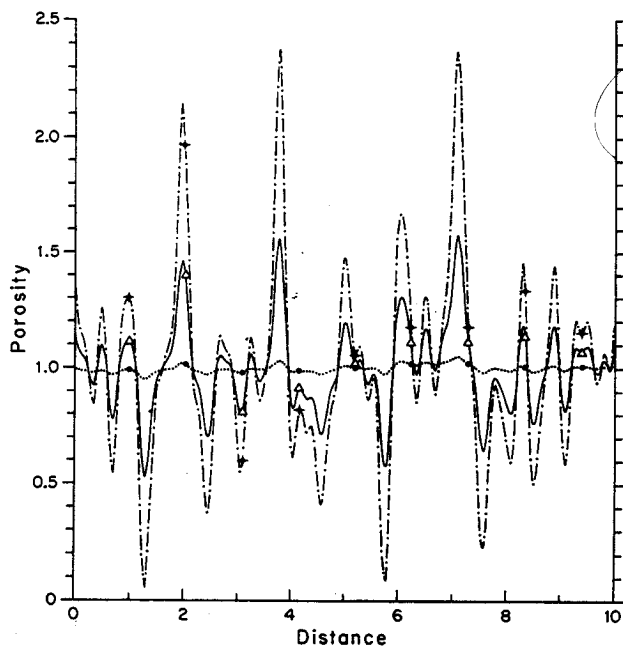


Fig. 4. Spatial and temporal evolution of an initial random distribution of minute deviations from the average porosity (a), and concomitant evolution of the pore fluid composition (b). Each positive deviation from the average porosity grows at first like the single deviation shown in Fig. 2, but then a competition between adjacent maxima sets in whereby a maximum, after having grown in the initial phase, starts to be eaten up by a neighboring maximum until it is annihilated. At this point the spacing between adjacent remaining maxima jumps up suddenly, and the competition between them greatly slows down. The process is termed here 'cascade' evolution. In (b) note that, as time passes, diffusion quickly smooths out the initial, sharp, closely-spaced, random deviations of pore fluid concentration and converts them into broader and more separated departures

deviations. In the satellite induction runs above we studied the evolution of a single local inhomogeneity, but in general we expect the initial texture to be a random deviation around the mean. The predicted evolution of such initial texture is shown in Fig. 4. We observe a dynamics of interference of local extrema leading to the generation of fairly regularly spaced stylolites, a feature often observed in rocks, as discussed in Sect. I. Note that this spacing is different from that generated in Fig. 2.

The dynamics here is somewhat different, and can be called "cascade" dynamics: small positive porosity deviations from the mean grow with time, as shown in Fig. 4a, but at some later time a competition between neighboring maxima sets in whereby some maxima grow at the expense of a neighboring maximum, which is annihilated. At this point the spacing between adjacent remaining maxima jumps up suddenly, or "cascades" up, and then the competition between them drastically slows down. (The annihilation of some maxima had not yet started by the time the run of Fig. 4a was terminated.) The spacing between adjacent remaining porosity maxima tends therefore to become frozen in as the dominant spacing between stylolites.

Figure 4b shows the spatial and temporal variation of the pore fluid concentration concomitant with the variation of porosity displayed in Fig. 4a. Note how, as time passes, diffusion quickly converts the initial, sharp, closely-spaced, random deviations from the average pore fluid concentration into broad, and more separated, departures that then grow positively or negatively.

V. Check of the Theory Against Natural Data

The order of magnitude of the spacing between adjacent stylolites can be calculated from Eq. (III.20) and compared to spacings observed in rocks for a check of

the kinetic theory developed in the preceding sections. The order of magnitude of the time needed for stylolite formation can also be estimated with Eq. (III.21). All the quantities in (III.20, 21) are known; their values or ranges of values are shown in Table 1. Before values are entered in (III.20, 21) we need to calculate α and β in (III.12, 13). The $\Delta\mu$ of (II.11, 12) is equivalent to Kamb's (1959, p 156) $\mu_{\perp} - \mu_0$ or $\mu_{\parallel} - \mu_0$, which can be calculated with his equations (13) and (14), which give the difference between the chemical potential of the crystal component in the fluid when the crystal is under uniaxial stress, and the chemical potential of the unstressed crystal. The equations apply strictly to rhombohedral minerals; the reader should see details in Kamb (1959). Using compliance values for quartz and calcite from Clark (1966) reproduced in Table 1 and taking from Sellier (1979, p 248) the reasonable values $p_x = 20-150$ bars and $p_z = 50-300$ bars under which stylolites are produced, $\Delta\mu$ reduces simply to $V_0 p_z$, where V_0 is the molar volume of the mineral in question, the quadratic terms being negligible.

Thus, $\alpha = \Delta\mu/RT \cong V_0 p_z/RT$. For quartz α can vary between 0.07 and 0.4, and β is negligible. Using extreme values in (III.20, 21) we obtain, using values in Table 1,

$$0.025 \text{ cm} \lesssim R_c^{\text{quartz}} \lesssim 2.8 \text{ cm} \quad (\text{V.1})$$

and

$$6,300 \text{ years} \lesssim T_c^{\text{quartz}} \lesssim 1.7 \times 10^6 \text{ years.} \quad (\text{V.2})$$

For calcite the prediction of spacing and time of formation yields far wider ranges, because k , the dissolution rate constant, appears to be a sensitive function of many factors such as pH, P_{CO_2} , ionic strength, and concentration of specific ions (Ca^{++} , Mg^{++} , PO_4^{3-} , Sc^{3+} , and probably many more, including organic inhibitors). Also, the dissolution rate law we have adop-

Table 1. Order of magnitude of quantities needed to calculate the typical spacing and typical time of formation of adjacent stylolites with Eqs. (III.20, 21).

	Quartz	Calcite	Other Quantities
V_0 , cm ³ /mole	22.7 ^a	36.9 ^a	$R = 8 \times 10^7$ erg/mole °K
$n^{-1/3}$, cm	$6 \times 10^{-3} - 2 \times 10^{-1}$ a	$6 \times 10^{-3} - 2 \times 10^{-1}$ d	$T = 300$ °K
k , cm/s	10^{-8} b	$10^{-3} - 10^{-10}$ c	$D_c = 10^{-5}$ cm ² /s ^e
ϵ	3.7×10^{-6} h	$3.7 \times 10^{-4} - 3.7 \times 10^{-9}$ i	$\phi = 0.01$ to 0.20
s_{11} , cm ² /dyne	1.28 ^g	1.13 ^g	$p_z = 5 \times 10^7$ to 3×10^8 dynes/cm ² f
s_{33} , cm ² /dyne	0.96 ^g	1.75 ^g	(50 to 300 bars)
s_{44} , cm ² /dyne	1.98 ^g	4.03 ^g	$p_x = 2 \times 10^7$ to 1.5×10^8 dynes/cm ² f
s_{12} , cm ² /dyne	-0.15 ^g	-0.37 ^g	(20 to 150 bars)
s_{13} , cm ² /dyne	-0.11 ^g	-0.43 ^g	
s_{14} , cm ² /dyne	0.45 ^g	0.91 ^g	

^a Molar volumes from Helgeson et al. (1978, Table 8)

^b Rate constant from Hurd and Theyer (1975)

^c Rate constants estimated in the text

^d Range of grain size in very fine to very coarse grained sediments; $n_p^{-1/3}$, which is the pore size, is taken as half the grain size e.g., Berner (1980)

^e Vertical and horizontal stresses needed to produce stylolites, from Sellier (1979, p 248)

^g Compliances from Clark (1966, Tables 7-12)

^h From the last equation of (III.1) along with a quartz solubility in water of 6 ppm

ⁱ From the last equation of (III.1) along with a calcite solubility in aqueous solution ranging in order of magnitude from 1 g/l to 10^{-5} g/l

ted in this study (see (II.7)) implicitly refers to minerals that dissolve into only one aqueous species (the concentration of which is X/ϕ). Equation (II.7) is therefore unsuitable to recover accurate k values from the calcite dissolution experiments of Berner and Morse (1974) and Sjöberg (1978), which were carried out in sea water or KCl solutions that in general had different concentrations of Ca^{++} and CO_3^{-} .

Nevertheless, bearing in mind (a) the order of magnitude of the rate constants obtained by Sjöberg (1978, p 22) from his own experiments and (b) the drastic depression of calcite dissolution rates caused by phosphate (Berner and Morse 1974), by scandium (Nestaas and Terjesen 1969), and by Mg^{++} , Ca^{++} and SO_4^{-} (Sjöberg 1978), we believe that k_{calcite} can range over many orders of magnitude (say, from about 10^{-3} cm/s down to 10^{-10} cm/s or less). Inserting these values into Eq. (III.20) along with values in Table 1 for average porosity, grain size and ion diffusion coefficients in carbonate rocks yields a broad range of expected spacings, from tens of centimeters down to 0.001 cm or even less. It is encouraging that this predicted range roughly agrees with observations on stylolite and microstylolite spacings in carbonate rocks (e.g., Stockdale 1922; Dunnington 1967) and on the delicate pressure solution textures described by Wanless (1979; see, for example, his Fig. 7b).

The order of magnitude of the typical time, T_c , for formation of stylolites in limestones is given by (III.21) using values in Table 1. Because the solubility of calcite in aqueous solution at low temperatures can vary from a maximum of $\sim 1\text{g/l}$ to essentially zero (depending on P_{CO_2} , pH, salinity, the sign and value of $M \equiv m_{\text{Na}^+} + m_{\text{K}^+} + 2m_{\text{Mg}^{++}} - m_{\text{Cl}^-} - 2m_{\text{SO}_4^{-}}$, and whether the system is open or closed to CO_2 - see for example Drever 1982, pp 44ff and Holland and Malinin 1979, pp 478ff), and because, as we have seen above, the calcite dissolution rate constant can also span several orders of magnitude, the range obtained for T_c is

$$3 \text{ hours} < T_c^{\text{calcite}} < 10^9 \text{ years.} \quad (\text{V.5})$$

The low end of this interval, even if it is too low by three orders of magnitude, opens up the tantalizing possibility that stylolites in a carbonate rock could be produced experimentally in a matter of months mostly by setting the conditions so that both the solubility and the dissolution rate constant are very high.

VI. Discussion and Conclusions

The kinetic theory presented accounts quantitatively for the generation of stylolites in a stressed rock having initially uniform texture. The stylolites arise through a feedback mechanism that works as follows: the larger the local porosity in a small volume of rock, the lower the cross sectional area, the greater the local stresses born by the mineral grains in that volume, and thus the higher the equilibrium concentrations of solutes in the local pore fluids. Diffusion then takes these solutes away to the rest of the rock where the porosity (and the equilibrium concentration) is lower. This in turn leads to further dissolution and further increase in porosity in an original region of higher porosity; the process accelerates itself.

A natural consequence of the theory, shown in the numerical simulations of Sect. IV, is the development of sets of stylolites with roughly regular spacing, which is a feature commonly observed in stylolitized rocks. From physical, thermodynamic, and kinetic quantities (porosity, grain size; temperature, stress, compliances, molar volume; dissolution rate constant) the theory allows us to calculate (see Sect. V) the orders of magnitude of stylolite spacing and time needed for stylolite formation. The predicted spacings (0.02–3 cm in quartz sandstones and 10^{-4} to 10^2 cm in carbonates) turn out to agree well with observed spacings in quartz arenites and carbonates. We think these results strongly support the kinetic theory presented above. The theory also explains the development of stylolites in rocks having initially non-uniform porosity, such as clastic rocks with graded bedding or silt/sand interlamination.

The mechanisms operating in the generation of stylolites in a sedimentary rock under stress - pressure solution, diffusion, and precipitation - are much the same ones operating in the formation of differentiated layering (Ortoleva et al. 1982, Strickholm et al. 1983). Indeed the spatial periodicity that is common to both differentiated layering and stylolites is accounted for by the same basic kinetic theory. The two phenomena, in spite of resulting from the same mechanisms, differ because of the great difference in initial porosity between metamorphic and sedimentary rocks. Complex crossover between metamorphic banding and stylolitization appears possible in multiminerale rocks with initially high porosity; at least, this is how we tentatively interpret the observation of authigenic illite in stylolites formed in quartz arenites of the Precambrian Flathead Sandstone of Montana (Shearer, ms. 1983), and in stylolites of the Silurian Green Pond Conglomerate of New Jersey (Thomson 1959, p 96). These effects could be described by generalizing the present theory to include two or more minerals.

As it stands now, the theory does not incorporate (1) the generation of columns and sockets, (2) the angle between the stylolites and the stress, (3) the closing together of the two blocks of rock separated by the stylolite, a compaction that must occur soon after, or roughly synchronously with, the pressure solution, (4) departures of grain shape from equant, and (5) precipitation of grains having preferred orientations with respect to the stylolite - as shown by Brown (1959).

Points (1) and (2) are three-dimensional features that may require a more complicated dependence of the equilibrium intergranular concentration on the local texture, as discussed in more detail by Ortoleva et al. (1982). As for point 3, the porosity profile predicted by our theory (see Figs. 2 and 4a), once the two blocks separated by the stylolite are brought into contact by the collapse that we postulate in Sect. I, reproduces well Harms and Choquette's (1965, plate 3C) observation that the porosity displays a minimum at the stylolite and increases away from it. The striations present on the sides of many stylolite teeth (Pettijohn, 1957, p 215) are good evidence for that collapse (see Introduction).

Point 4 involves the breakdown of the assumption that grains are at all times equant. It is commonly observed that grains next to a stylolite are roughly

tabular and have their short dimension perpendicular to it. Our work in progress describes departures from equidimensionality, incorporates them into the theory (which requires separate bookkeeping for the grain dimensions in the directions parallel and normal to the applied stress), and suggests that the shortening of grains at right angles to the stylolites tends to *oppose* the stylolite instability and also leads to rock compaction.

To take into account preferred orientation of grains (point 5) the present theory could be generalized by using the formalism of Merino and Ortoleva (1980) to incorporate the distribution of crystal-axis orientations. Finally, another relevant improvement in the theory would be to account for the concentration of crystal imperfections, notably dislocations, induced by the stress. The equilibrium constant would then not only depend on the instantaneous local texture but also on the defect density. The latter would obey an equation of motion reflecting a texture-dependent rate of defect formation.

In reexamining our assumptions it is clear that the formation of stylolites does not depend *in detail* on our choice (represented by Eq. III.6) of the effective dependence of the equilibrium constant on local porosity; the essential feature is that the equilibrium constant, under an applied stress, increases with increasing porosity. The rough agreement of our qualitative and quantitative results with observations suggests that the theory presented above constitutes a first and promising step in developing a quantitative kinetic theory of the spontaneous generation and spacing of stylolites in stressed rocks.

Note Added in Proof

The kinetic theory proposed above refers to the average pressure-solution/mass-transfer feedback among *small regions that are, say, 4 to 6 grain-lengths across, or that contain on the order of 50 to 150 grains*. Because stress-driven chemical-potential differences among the several facets of a grain have been here averaged over its surface area (see text between Eqs. (II.10) and (II.11)) and because grains have been assumed to remain equant throughout stylolitization (Sect. I.B), the theory, as it stands here, leaves out the details of the pressure-solution behavior on a single-grain length scale. Undoubtedly, this pressure solution on a grain scale tends to reduce local porosity and local stress, thereby opposing the feedback proposed here.

The present kinetic theory is consistent with the isotopic data of Hudson (Geology 3 [1975] 19–22) and with the excellent petrographic observations of Wong and Oldershaw (J Sediment Petrol 51 [1981] 507–520): both studies (which RGC Bathurst pointed out to us) conclude that burial cementation is carried out mostly with cement derived locally by pressure solution.

We are very grateful to RGC Bathurst and Craig H Moore for their enlightening critical comments.

References

Alvarez W, Engelder T, Lowrie W (1976) Formation of spaced cleavage and folds in brittle limestone by dissolution. Geology 4:698–701

- Amstutz GC, Park WC (1967) Stylolites of diagenetic age and their role in the interpretation of the southern Illinois fluorspar deposits. Miner Deposita 2:44–53
- Bathurst RGC (1975) Carbonate sediments and their diagenesis. Elsevier Develop Sedimentology Ser, No. 12 (second enlarged ed.), 677 p
- Bathurst RGC (1980) Deep crustal diagenesis in limestones. Rev Inst Invest Geológicas, Diputación Provincial, Univ Barcelona 34:89–100
- Berner RA (1980) Early diagenesis. p241. Princeton Univ Press
- Berner RA, Morse JW (1974) Dissolution kinetics of calcium carbonate sea water – IV. Theory of calcite dissolution. Am J Sci 274:108–134
- Bjorlykke K (1979) Cementation of sandstones: a discussion. J Sediment Petrol 49:1358–1359
- Brown WWH (1959) The origin of stylolites in the light of a petrofabric study. J Sediment Petrol 29:254–259
- Buxton TM, Sibley DF (1981) Pressure solution features in a shallow buried limestone. J Sediment Petrol 51:19–26
- Clark SP (1966) Handbook of Physical Constants. Geol Soc Am Mem 97:p507
- Drever JI (1982) The geochemistry of natural waters. Prentice-Hall, Englewood Cliffs, NJ, p 388
- Dunnington HV (1967) Aspects of diagenesis and shape change in stylolitic limestone reservoirs. Seventh World Petroleum Congress Proceedings (Mexico) 2:339–352
- Enos P, Sawatsky LH (1981) Pore networks in Holocene carbonate sediments. J Sediment Petrol 51:961–985
- Feeney R, Schmidt SL, Strickholm P, Chadam J, Ortoleva P (1983) Periodic precipitation and coarsening waves: Applications of the competitive particle growth model. J Chem Phys (in press)
- Fletcher RC, Pollard DD (1981) Anticrack model for pressure solution surfaces. Geology 9:419–424
- Garrels RM, Christ CL (1965) Solutions, Minerals and Equilibria. Harper and Row, New York, p450
- Harms JC, Choquette PW (1965) Geologic evaluation of a gamma-ray porosity device. Trans Soc Profess Well Log Analysts, 6th Ann. Logging Symposium, Dallas, Texas, C, 1–37
- Heald MT (1955) Stylolites in sandstones. J Geol 63:101–114
- Heald MT (1959) Significance of stylolites in permeable sandstones. J Sediment Petrol 29:251–253
- Helgeson HC, Delany JM, Nesbitt HW, Bird DK (1978) Summary and critique of the thermodynamic properties of rock-forming minerals. Am J Sci 278-A:1–229
- Holland HD, Malinin SD (1979) The solubility and occurrence of non-ore minerals. In: Geochemistry of Hydrothermal Ore Deposits, Barnes HL (ed), Wiley, 2nd ed. pp461–508
- Hurd DC, Theyer F (1975) Changes in the physical and chemical properties of biogenic silica from the Central Equatorial Pacific – I. Solubility, specific surface area, and solution rate constants of acid-cleaned samples. In: Analytical Methods in Oceanography Gibb RP, Jr, (ed), Advances in Chemistry Series, No 147, Am Chem Soc:211–230
- Kamb B (1959) Theory of preferred crystal orientation developed by crystallization under stress. J Geol 67:153–170
- Lerman A (1979) Geochemical processes. New York: Wiley p481
- Manten AA (1966) Note on the formation of stylolites. Geol Mijnbouw 45:269–274
- Merino E, Ortoleva P (1980) Temporal development of fabric in uniaxially stressed polycrystalline media – a theory. Contrib Mineral Petrol 71:429–435
- Nestaas I, Terjesen SG (1969) The inhibiting effect of scandium ions upon the dissolution of calcium carbonate. Acta Chem Scand 23:2519–2531

- Ortoleva P, Merino E, Strickholm P (1982) A kinetic theory of metamorphic layering in anisotropically stressed rocks. *Am J Sci* 282:617-643
- Park WC, Schot EH (1968) Stylolites: Their nature and origin. *J Sediment Petrol* 38:175-191
- Pettijohn FJ (1957) *Sedimentary Rocks* (2nd ed). Harper and Row, New York, p718
- Robin P-YF (1978) Pressure solution at grain-to-grain contacts. *Geochim Cosmochim Acta* 42:1383-1389
- Rutter EH (1976) The kinetics of rock deformation by pressure solution. *Phil Trans R Soc Lond A* 283:203-219
- Sellier E (1979) Contribution à l'étude pétrologique expérimentale de la genèse des stylolithes dans les formations calcaires du bassin d'Aquitaine. Docteur ès Sciences Thesis, University of Bordeaux III, p300
- Shearer JN (1983) Petrology of the Precambrian Flathead Formation of Montana. PhD Dissertation, Indiana University, ms (in progress)
- Sjöberg EL (1978) Kinetics and mechanism of calcite dissolution in aqueous solutions at low temperatures. *Stockholm Contributions in Geology* 32:p92
- Stockdale PB (1922) Stylolites: Their nature and origin. *Indiana University Studies* 9:p97
- Strickholm P, Merino E, Ortoleva P (1983) The self-organization of differentiated layering. Submitted to *J Geophys Res*
- Thomson A (1959) Pressure solution and porosity. In: *Silica in Sediments*, Ireland HA (ed) pp 92-110, *Soc Econ Paleont Mineral Spec Pub* 7
- Tremolières P, Reulet J (1978) Influence des déformations tectoniques sur les caractéristiques pétrophysiques matricielles des réservoirs calcaires. *Rev Inst Français du Pétrole* 33:331-348
- von Rosenberg DU (1969) *Methods for the numerical solution of partial differential equations*. New York: American Elsevier Publishing Co, Inc
- Wanless HR (1979) Limestone response to stress: pressure solution and dolomitization. *J Sediment Petrol* 49:437-462

Received September 16, 1981; Accepted March 1, 1983